

Supporting Information : Effects of counterion size and backbone rigidity on dynamics of ionic polymer melts and glasses

Yao Fu,^{1,2} Vera Bocharova,³ Mengze Ma,⁴ Alexei P. Sokolov,^{3,5} Bobby G. Sumpter,^{2,6} and Rajeev Kumar ^{*2,6}

¹*Department of Aerospace Engineering and Engineering Mechanics,
University of Cincinnati, Cincinnati, OH-45220*

²*Center for Nanophase Materials Sciences,
Oak Ridge National Laboratory, Oak Ridge, TN-37831*

³*Chemical Sciences Division, Oak Ridge National Laboratory, Oak Ridge, TN-37831*

⁴*Department of Mechanical and Materials Engineering,
University of Cincinnati, Cincinnati, OH-45220*

⁵*Department of Chemistry, University of Tennessee, Knoxville, TN - 37996*

⁶*Computational Sciences and Engineering Division,
Oak Ridge National Laboratory, Oak Ridge, TN-37831*

(Dated: June 16, 2017)

* To whom any correspondence should be addressed, Email : kumarr@ornl.gov

I. RADIAL DISTRIBUTION FUNCTIONS

Typical snapshots of a single chain and a polymer melt with neutralizing counterions are shown in Fig. S1.

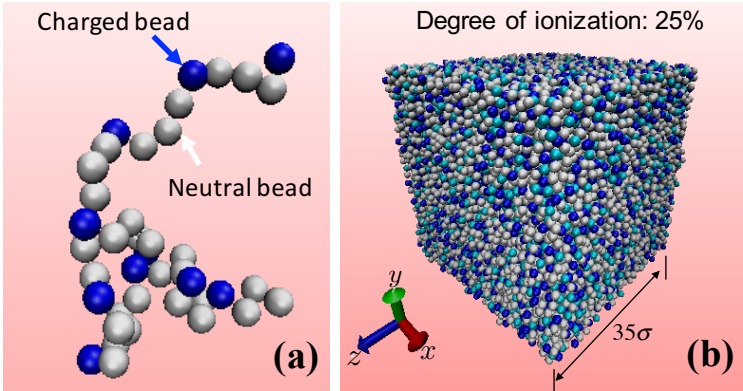


Fig. S1: Snapshot of a charged homopolymer at 25% degree of ionization in (a) single chain and (b) bulk; neutral monomers, charged monomers and the counterions are presented in white, blue, and cyan, respectively

The radial distribution functions for charged monomer-charged monomer ($g_{cm-cm}(r)$), charged monomer-counterion ($g_{cm-ci}(r)$) and counterion-counterion ($g_{ci-ci}(r)$) pairs are shown in Fig. S2 for the smallest ($r_{ci} = 0.05 \sigma$) and the biggest ($r_{ci} = 0.50 \sigma$) counterions. In particular, structural changes due to an approach to the glass transition temperature are revealed in Fig. S2, which corresponds to the chains simulated without the inclusion of angular potentials.

II. GLASS TRANSITION TEMPERATURE AND FRACTION OF IMMOBILE MONOMERS

The glass transition is directly related to the drastic increase of segmental relaxation time or the decrease of segmental mobility and the fraction of immobile monomers can serve as a good indicator of an approach to the glass transition process. Therefore, to further confirm the change of T_g with r_{ci} , the number of immobile monomers at a chosen temperature around the estimated T_g was analyzed. The flexible chains with $\epsilon_r = 10$ at $T^* = 0.5$ were chosen as

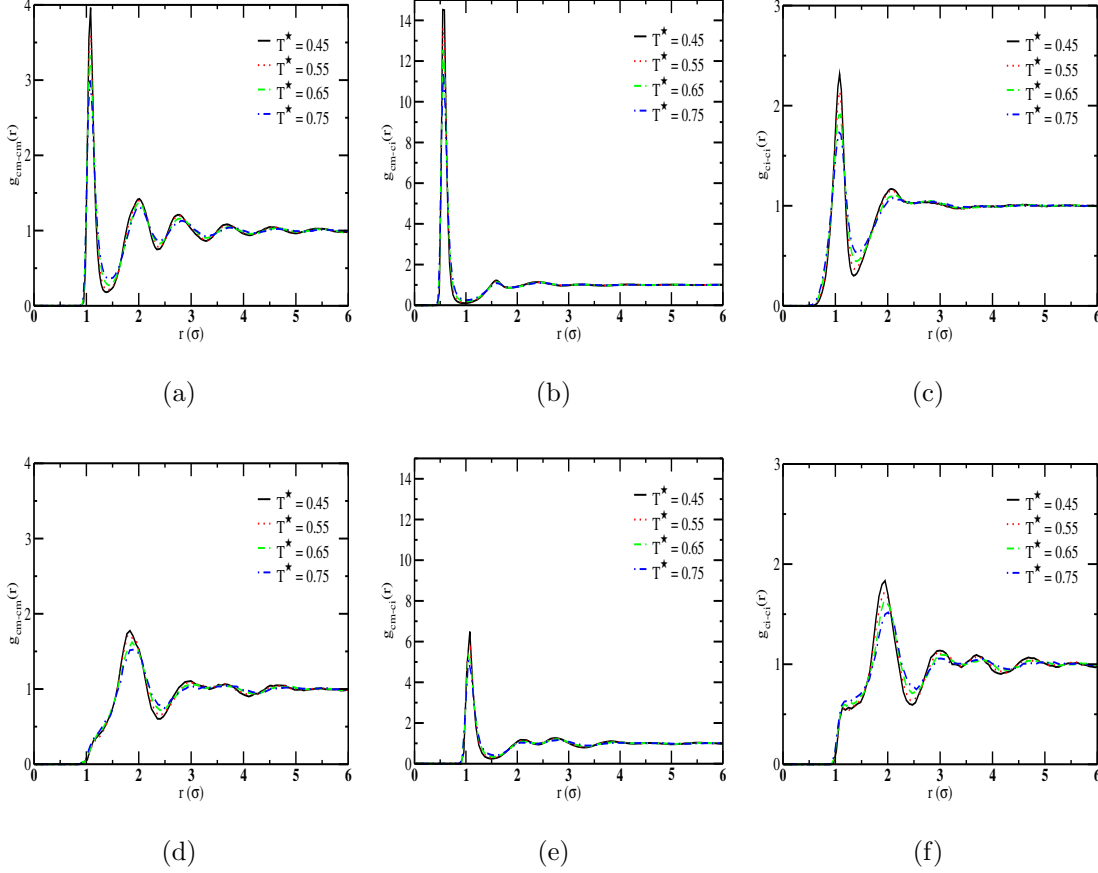


Fig. S2: Radial distribution functions of the charged monomer-counterion $g_{cm-ci}(r)$, charged monomer-charged monomer $g_{cm-cm}(r)$ and counterion-counterion $g_{ci-ci}(r)$ pairs in the polymer melts containing the flexible chains at $\epsilon_r = 10$. Top and bottom panels correspond to $r_{ci} = 0.05\sigma$ and $r_{ci} = 0.50\sigma$, respectively.

very similar tendency was observed despite the semi-flexibility and the dielectric constant. Following the algorithm by Starr *et al.* [1], the immobile monomers were identified as the “caged monomers”. The cage size was defined as $r_{cage} \equiv \langle r^2(t_{cage}) \rangle^{1/2}$, where t_{cage} is the time scale at which the logarithmic derivative, $d(\ln\langle r^2(t) \rangle)/d(\ln t)$, exhibits a minimum. As expected, the fraction of immobile (or caged) monomers, i.e., monomers with displacement less than r_{cage} , was found to gradually reduce with time (Fig. S4(a)). In particular, an initial fast decay of the fraction of immobile monomers followed by a slower decay was observed. Changes in the rate of decay due to the changes in the counterion radii result from the cluster redistribution manifested in the temperature dependent radial distribution functions and the maximum number of monomers in the cluster of the immobile monomers shown in Fig. S4(b). For the cluster analysis, we have used a cut-off distance of 1.5σ . It should be

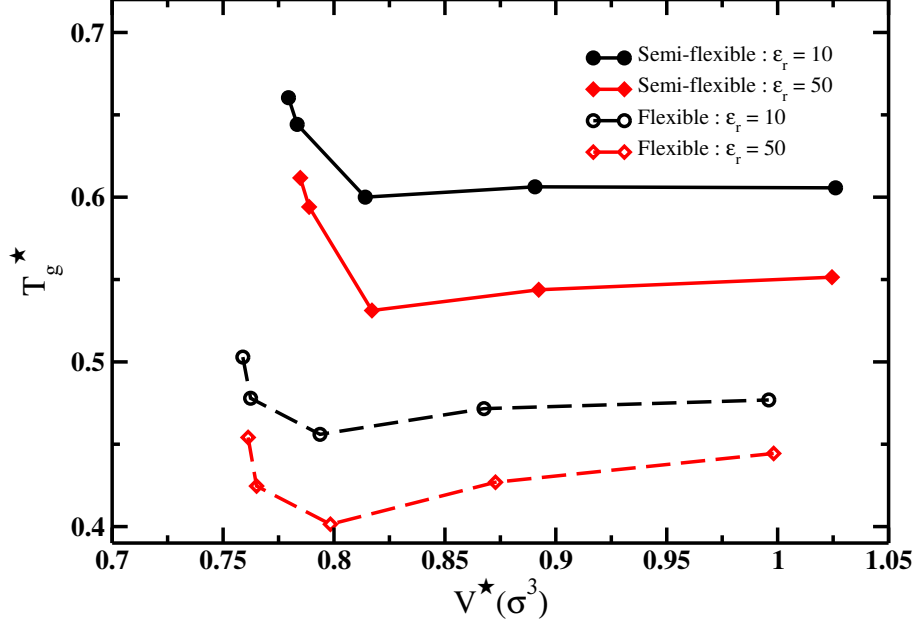


Fig. S3: Glass transition temperature, T_g^* , as a function of the specific volume.

clear from Fig. S4(b) that bigger counterions tend to reduce the number of monomers in clusters at longer times. However, characteristic cage size for a monomeric bead increases slightly with an increase in r_{ci} , which means that the monomeric beads can traverse further.

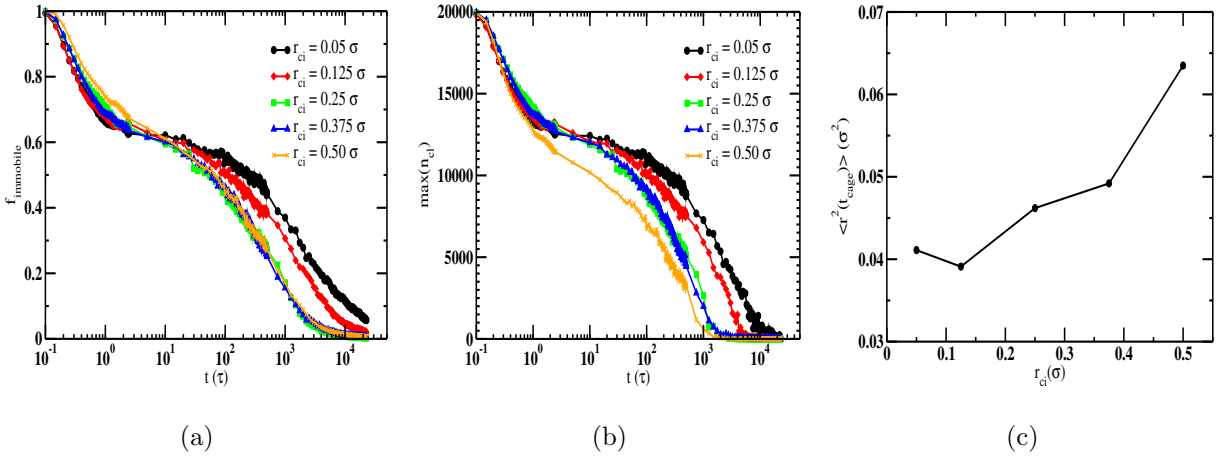


Fig. S4: Evolution of the fraction of immobile monomers (a), maximum cluster size, n_{cl} , (b) with time at different counterion sizes in the flexible ionic homopolymers at $\epsilon_r = 10, T^* = 0.5$. Panel (c) shows the characteristics size of the cage for a monomeric bead.

III. MEAN SQUARED DISPLACEMENT (MSD), AVERAGE VORONOI VOLUME, FREE VOLUME AND DIFFUSION CONSTANTS

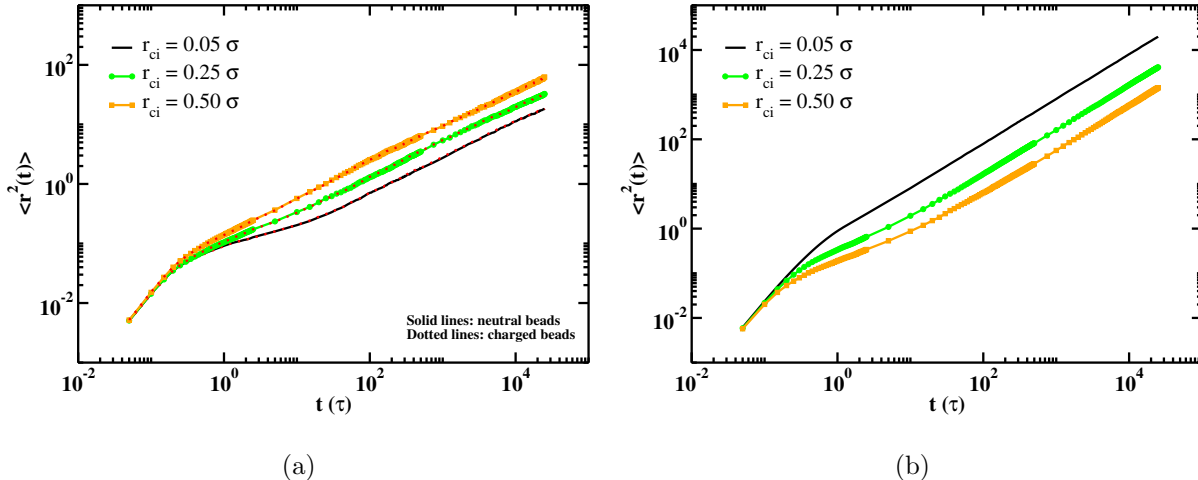


Fig. S5: MSD of the monomers (a) and counterions (b) in semi-flexible ionic homopolymers at $\epsilon_r = 50, T^* = 0.8$.

In order to understand the role of free volume in ion transport, the Voronoi volume of the counterions was computed and the free volume was obtained by subtracting the respective volume of the counterions defined as $v_{ci} = \frac{4}{3}\pi r_{ci}^3$. The same analysis was done for the monomeric beads on the chains and the results are presented in Fig. S6. It is found that the average Voronoi volume as well as the free volume per counterion and monomer are higher in the melts containing semi-flexible chains. An increase in r_{ci} leads to increase in the average Voronoi volume and the free volume. Small decrease in the free volume for $r_{ci} = 0.50\sigma$ results from getting closer to T_g^* due to the increase in T_g^* as shown in Fig. S3.

[1] F. W. Starr, J. F. Douglas, and S. Sastry, The Journal of Chemical Physics 138, 12A541 (2013);
doi: 10.1063/1.4790138

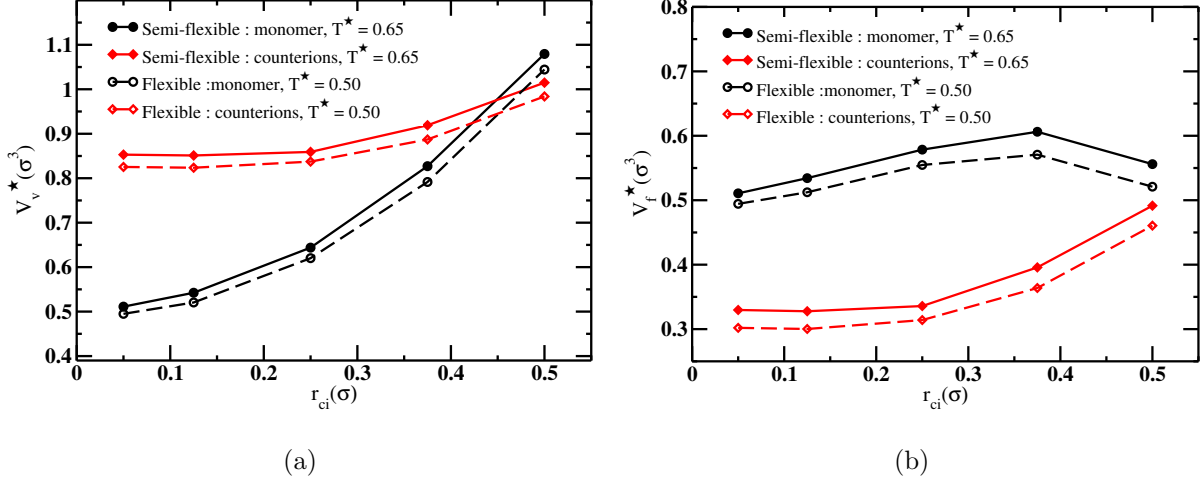


Fig. S6: (a) Variation of the average Voronoi volume (V_v^*) with counterion radius, r_{ci} at $\epsilon_r = 10$, and the corresponding free volume (V_f^*) changes are shown in panel (b). The free volumes of a counterion and the monomeric bead are defined as the average Voronoi volume minus the counterion volume ($= 4\pi(r_{ci}/\sigma)^3/3$) and monomeric volume ($= 4\pi(0.5)^3/3$), respectively.

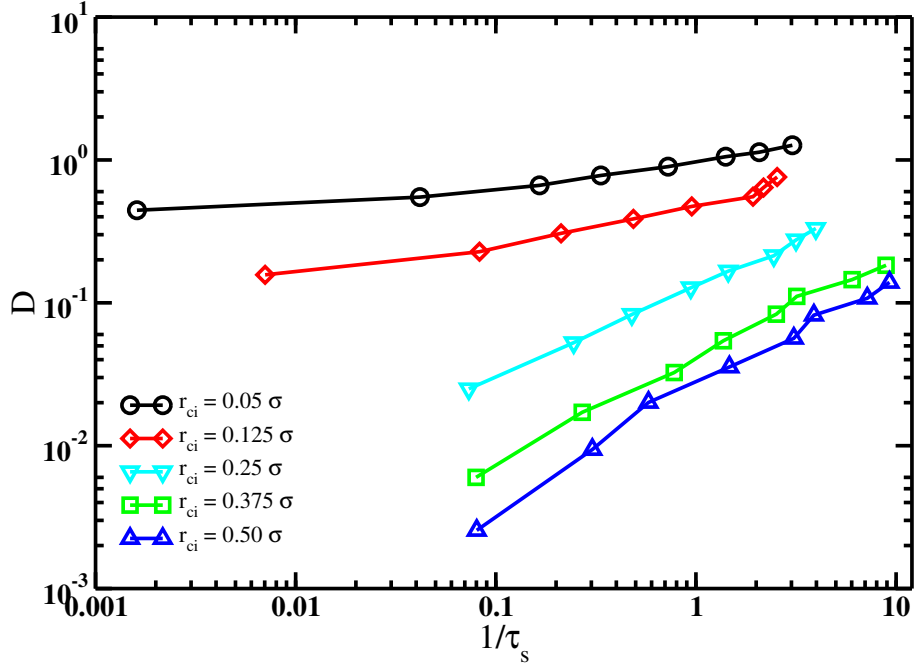


Fig. S7: Effects of size of the particles on the relation between diffusion constant and the segmental relaxation time τ_s for the chains simulated without the angular potential after deliberately switching off the electrostatic interactions.